Department of AERONAUTICS and ASTRONAUTICS

STANFORD UNIVERSITY

Final Report

October 1, 1982 - September 30,1983

on

PHOTODIAGNOSTICS OF TURBULENT FLOWS USING LASER-INDUCED FLUORESCENCE

Cooperative Agreement NCC 2-82

Submitted to the

National Aeronautics and Space Administration

Ames Research Center

Moffett Field, California 94035

R. L. McKenzie - Technical Officer

by the

Department of Aeronautics and Astronautics

Stanford University

Stanford, California

Principal Investigator: Daniel Bershader

Research Associate: Kenneth P. Gross

December 1983

Abstract

The goal of this project is the development of an optical probe technique that will allow remote measurements of temperature (and density), along with their time-dependent fluctuations, to be made in a supersonic turbulent wind tunnel flow. The approach chosen for this study focuses on using laser-induced fluorescence from nitric oxide which has been seeded into the flowing gas medium (nitrogen) at low concentrations. The fluorescence emission intensity following laser excitation of the nitric oxide (NO) ground state rotational levels is then related to thermodynamic quantities of the bulk fluid.

Summary of Research

Research progress and results culminating over the reporting period are described in detail in the articles and pre-prints included at the end of this report (references 1-3). A synopsis of the work follows.

A laser-induced fluorescence (LIF) probe technique, using two-photon excitation in NO/N_2 mixtures, has been developed [1] for supersonic turbulent flow studies, and a preliminary proof of concept demonstration [2] has been completed for a simple two-dimensional boundary layer flow at Mach 2. The method has been successful in measuring the average temperature profile through a classical boundary layer, and the magnitudes of the temperature fluctuations about the average values. The instantaneous temperature measurement sensitivity was 3-4 % for an NO

concentration of 300 parts per million (ppm). For typical flow conditions (0.5 - 1.0 atm, 150 - 300 K, 300 ppm NO), we regard these results as indicative of the fundamental limit of sensitivity that can be obtained by the present methodology using the two-photon excitation method. The primary limitation is imposed by an anomalously large optical Stark effect in the two-photon spectrum of NO which manifests itself as a broadening and merging of the spectroscopic lines used for the measurement. This phenomena which scales linearly with the laser intensity, forces one to minimize the laser power density, with a resultant increase in photon-statistical signal noise. Efforts to understand the origin of this effect in nitric oxide have resulted in a collaborative endeavor with the Computational Chemistry branch at Ames (see reference 3 for details). It is believed that a firm understanding of this phenomena may be of importance for the use and design of other laser-based diagnostic methods that depend on the use of high-power pulsed laser sources.

Additionally over the past year, work has been initiated to refine and extend the present capabilities of the LIF/NO measurement scheme by investigating the use of single-photon excitation of NO as an alternative to the two-photon method. This re-evaluation of the laser methodology was prompted primarily by the limitations resulting from the Stark effect. Preliminary work suggests that for nitric oxide concentrations around 100 ppm, an rms temperature measurement noise in the 1 - 2 % range is feasible. Moreover, the lower level of fluorescence signal noise afforded by this method will allow the simultaneous

determination of density with comparable noise levels, thereby allowing pressure to be non-intrusively measured as well. The advantages of the single-photon excitation scheme are numerous: a) negligible stark shift; b) fluorescence s/n >> 100; c) comparable sensitivity for measurement of temperature and density; d) measurement of pressure; e) lower concentrations of NO (reduced toxicity). The disadvantages or problem areas that must be confronted include: a) experimental setup more complex; b)finite absorption of laser intensity for moderate optical depths; c) partial saturation of electronic transitions. Work along these lines is in progress to validate the accuracy and applicability of the single-photon method for making simultaneous measurements of temperature, density and pressure in turbulent flow regimes that are of interest in modern fluid-dynamics research.

References (see attached)

1. "Single-pulse gas thermometry at low temperatures using two-photon laser-induced fluorescence in NO-N_2 mixtures", K. P. Gross and R.L. McKenzie, Opt. Lett. 8, 368 (1983).
2. "Remote measurements of fluctuating temperatures in a supersonic turbulent flow using two-photon laser-induced fluorescence", K. P. Gross and R. L. McKenzie, submitted for presentation at the AIAA 17th Fluid Dynamics, Plasma Dynamics, and Lasers Conference to be held in Snowmass, Colorado, June 25 - 27, 1984.
3. "Optical Stark effect in the two-photon spectrum of NO", W. M. Huo, K. P. Gross, and R. L. McKenzie, to be submitted for publication in Physical Review Letters.

REFERENCE 1

REPRINT - SENT TO AIAA - FEBRUARY 28, 1984

Remote Measurements of Fluctuating Temperatures in a Supersonic Turbulent Flow Using Two-Photon Laser-Induced Fluorescence

by

K.P.Gross

Polyatomics Research Institute, 1101 San Antonio Rd., Suite 420, Mountain View, CA., 94043

and

R.L.McKenzie

NASA Ames Research Center, N-229-1, Moffett Field CA., 94035

A laser-induced fluorescence (LIF) technique has been developed that provides a practical means of nonintrusively measuring the fluctuating temperatures in low-temperature turbulent flows. In this paper, we review the capabilities of the method and report its application to a simple two-dimensional turbulent boundary layer flow at Mach 2. We show the results of remote measurements of the average temperature distribution through the boundary layer and the magnitudes of temperature fluctuations about their average values. To our knowledge, these data are the first of their kind obtained by nonintrusive means with spatial and temporal resolution adequate for turbulent boundary layer analyses.

The method, described in detail previously(1), requires that the flow be seeded with a low concentration of nitric oxide (NO). It relies on the ultraviolet fluorescence following two-photon excitation of two ro-vibronic transitions in the NO Gamma band. Each excitation is induced by a separate tunable dye laser tuned to the transition of interest. The two dye lasers are pumped by a common Nd:YAG laser but at slightly separated times following each pump

laser pulse. The subsequent double-pulse waveforms depicting the combined broad-band fluorescence from both excitations are then recorded, normalized by similar data from a non-flowing reference cell at known temperature, and related to the rotational temperature of the ground-state NO molecule. The rotational temperature of NO is taken to be closely coupled to the kinetic temperature of the gas mixture, thus providing a temperature measurement with each pump laser pulse. The temporal resolution of the measurement is approximately 125 nsec and it is obtained within a sample volume having dimensions less than 1 mm.

The windtunnel used for these experiments is a small blowdown facility that is capable of handling toxic gases such as NO. Nitric oxide concentrations up to 300 ppm were used, mixed with dry nitrogen. The test section is a rectangular Mach 2 nozzle with a 25 X 64 mm exit, followed by a slightly diverging channel, 762 mm in length from the nozzle throat to the optical ports. Optical access to the flow for the lasers was obtained through 50 mm diameter quartz windows on each side of the channel while fluorescence was observed through a similar window in the top of the channel. At a stagnation pressure of 3.5 atmospheres, the test section contained a fully-turbulent boundary layer filling the upper and lower thirds of its 33 mm height and had an inviscid core flow in the center.

The optical arrangement is illustrated in Fig. 1. Two grating-tuned dye lasers are simultaneously pumped at 10 Hz by the third-harmonic output of an Nd:YAG laser. The portion of the 355 nm pump beam directed to the second dye laser was optically delayed, giving a temporal separation of 125 nsec between dye laser pulses.

The first and second dye lasers were tuned, respectively, to

the J"=19 1/2 and J"=7 1/2, S11+R21 two-photon transitions in the NO Gamma(0,0) band. The two beams were combined collinearly, focused by a common 500 mm focal length lens, and partitioned into the windtunnel and reference paths. The focal spot size was about 0.5 mm.

The broad-band fluorescence from both the windtunnel and the reference cell was collected with nearly identical f/1 fused silica optics, nominally filtered with UV transmitting short-wave-pass filters, and imaged through apertures that limited observation of both sample volumes to a 1 mm region centered on the laser beam focal point. The fluorescence waveforms from each source were detected by solar-blind photomultipliers sensitive in the spectral range 225-330 nm and recorded by Tektronix 7912AD transient digitizers interfaced to an HP-1000 computer.

As described in Ref. 1, the data analysis leading to a temperature value for each pump laser pulse requires knowing the ratio of broad-band fluorescence energies resulting from each excitation. The ratio is obtained from each double-pulse waveform by fitting it to a six-parameter function derived for an exponentially decaying emitter driven by an excitation pulse with a Gaussian temporal profile. The two pulses in each waveform are then deconvolved and their individual integrals computed. The integral of each pulse is assumed to be linearly proportional to the total fluorescence energy resulting solely from its corresponding laser excitation, with account taken of the laser spectral width and all collision-broadened molecular transitions falling within the excitation bandwidth.

Figure 2 shows an overlay of some experimental waveforms and

their functional fits. In each example, the first pulse results from excitation of the J"=19 1/2 transition using excitation energies in the range from 1.5 to 2.0 mJ. The second pulse is from excitation of the J"=7 1/2 transition using approximately 0.5 mJ. Under these conditions, the noise seen in the waveforms is due principally to photon statistics with signal-to-noise ratios in the range of 25-50 for the windtunnel and 50-100 for the reference cell.

Prior to its windtunnel application, the instrumental uncertainty of the method was evaluated in a cooled non-flowing cell at conditions duplicating those expected in the windtunnel. The cell contained thermocouples located close to the laser sampling point that provided an independent measurement of the local temperature in the gas mixture. A comparison of temperature measurements in the cell over the range 155-295 K are shown in Fig. 3. The average temperatures calculated from 50 laser pulses are represented by the symbols. The error bars indicate the corresponding RMS deviation from each average value. Generally, the average spectroscopic temperatures agree with the thermocouples to within +/- 2 %, whereas the single-pulse temperatures varied between 2.5-4.0 % RMS for each data set.

The results of preliminary windtunnel measurements are illustrated in Figures 3 and 4. Figure 3 shows the variation of average temperatures obtained by the LIF technique as the measurement point is traversed from the channel centerline to a position approximately 0.7 mm from the wall. The filled symbols represent averages accumulated during 15 second runs with account taken of the declining stagnation temperature that is characteristic of all blowdown windtunnels. The open symbols are temperatures

implied from a pitot probe survey at the same conditions. The LIF average temperatures agree with the pitot values within +/- 2 % at all locations.

Figure 4 compares the RMS magnitudes of temperature fluctuations obtained by the LIF technique with similar measurements made using hot-wire probes in the same channel (open symbols) and with hot-wire measurements in a larger facility at similar conditions (dashed line). At this time, the cause of the apparent lack of agreement is unclear but the LIF measurements are judged to be less subject to interpretation than those from the intrusive hot-wire probes.

We believe that this nonintrusive laser-induced fluorescence technique offers new opportunities in basic turbulent flow research by providing measurement capabilities that were not possible previously. We have strong indications from other laboratory results that we will soon be able to extend it to include simultaneous temperature and density measurements, thus allowing pressure fluctuations to be obtained nonintrusively.

1. R.L.McKenzie and K.P.Gross, Two-Photon Excitation of Nitric Oxide Fluorescence as a Temperature Indicator in Unsteady Gasdynamic Processes , Appl. Optics. 20 ,2153,(1981)

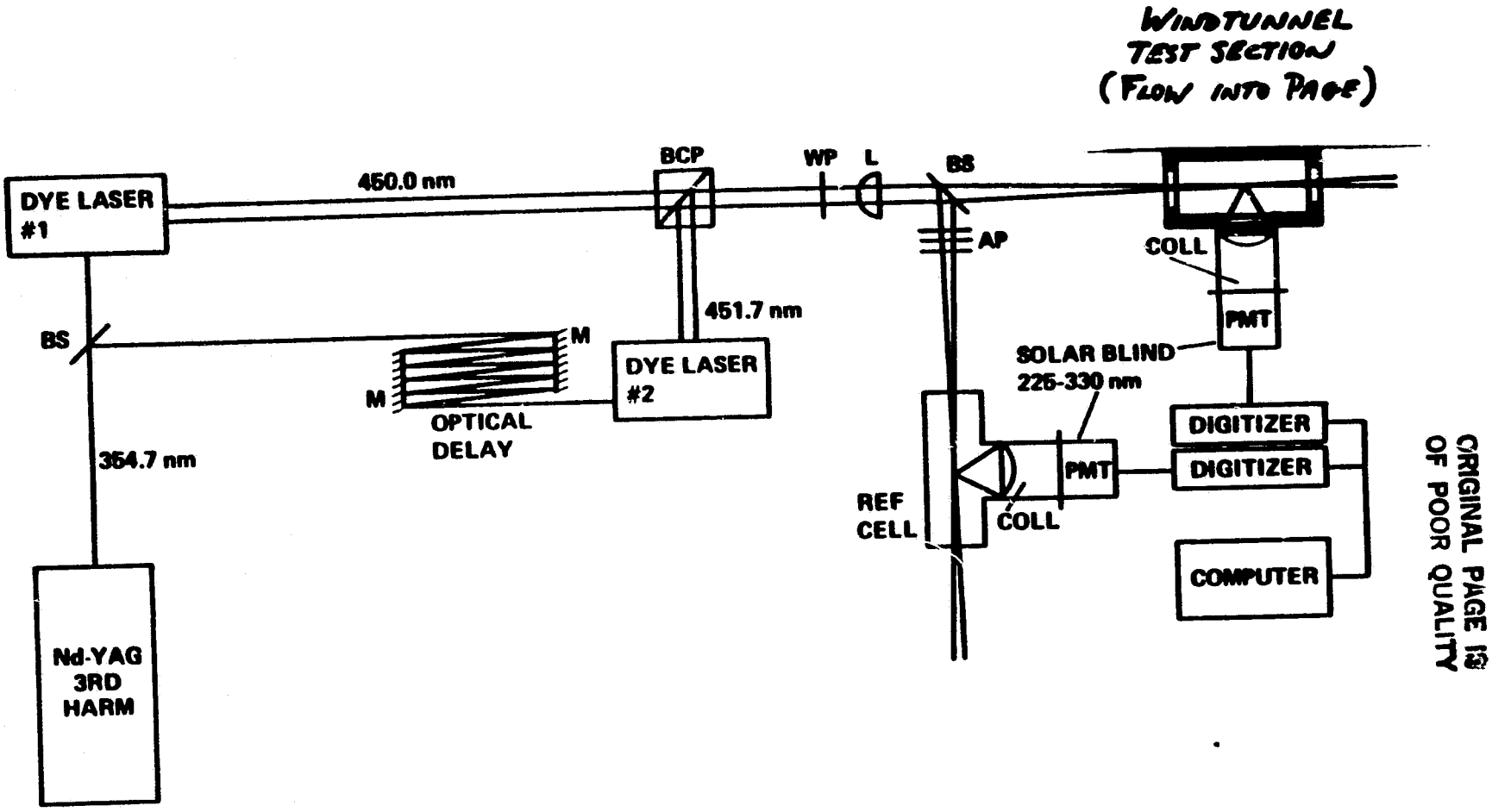

Fig. 1. Schematic of the experimental arrangement: BCP, beam-combining polarizer cube; WP, half-wave plate; L, lens; BS, beamsplitter; M, mirror; AP, attenuation plates; COLL, collection system; PMT, photomultiplier.

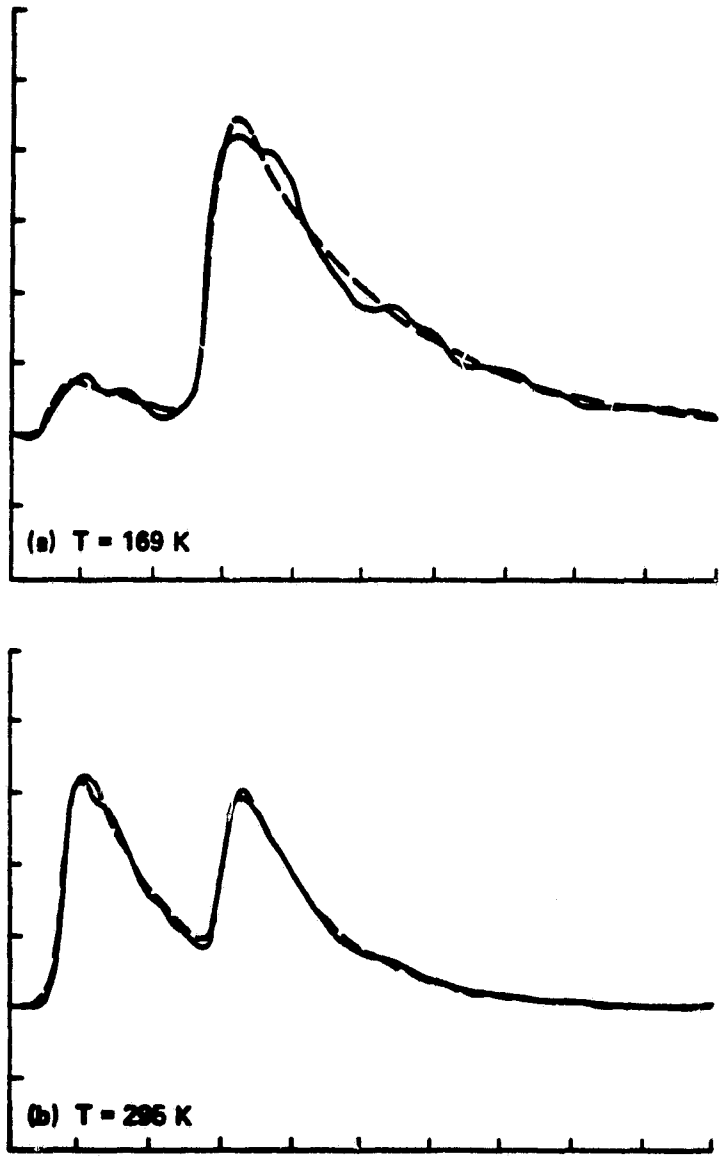

Fig. 2. Dual-pulse fluorescence waveform (solid line) and computer-fitted function (dashed line): (a) cold sample cell with 300 ppm NO in 0.5 atm N_2; (b) room-temperature reference cell with 1200 ppm NO in 0.5 atm. N_2. First pulse is fluorescence from the $S_{11} + R_{21}(19\ 1/2)$ excitation; second pulse is from the $S_{11} + R_{21}(7\ 1/2)$ excitation. Vertical amplifier bandwidth, 20 MHz; sweep, 50 nsec/div.

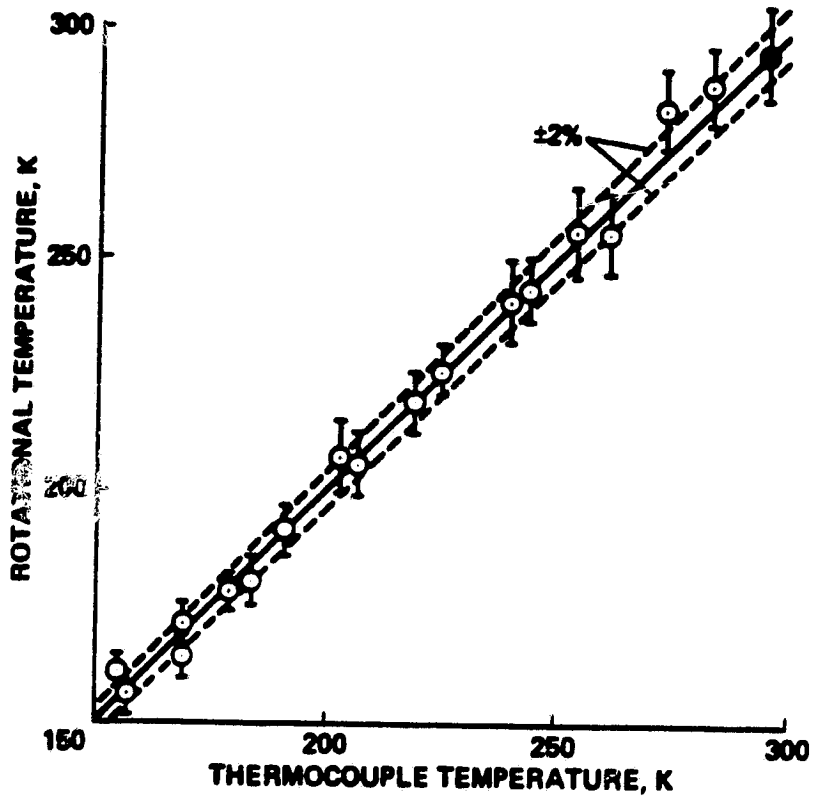

Fig.3 Comparison of measured rotational temperature and thermocouple temperature. Cell mixture: 300 ppm NO in 0.5 atm. N_2.

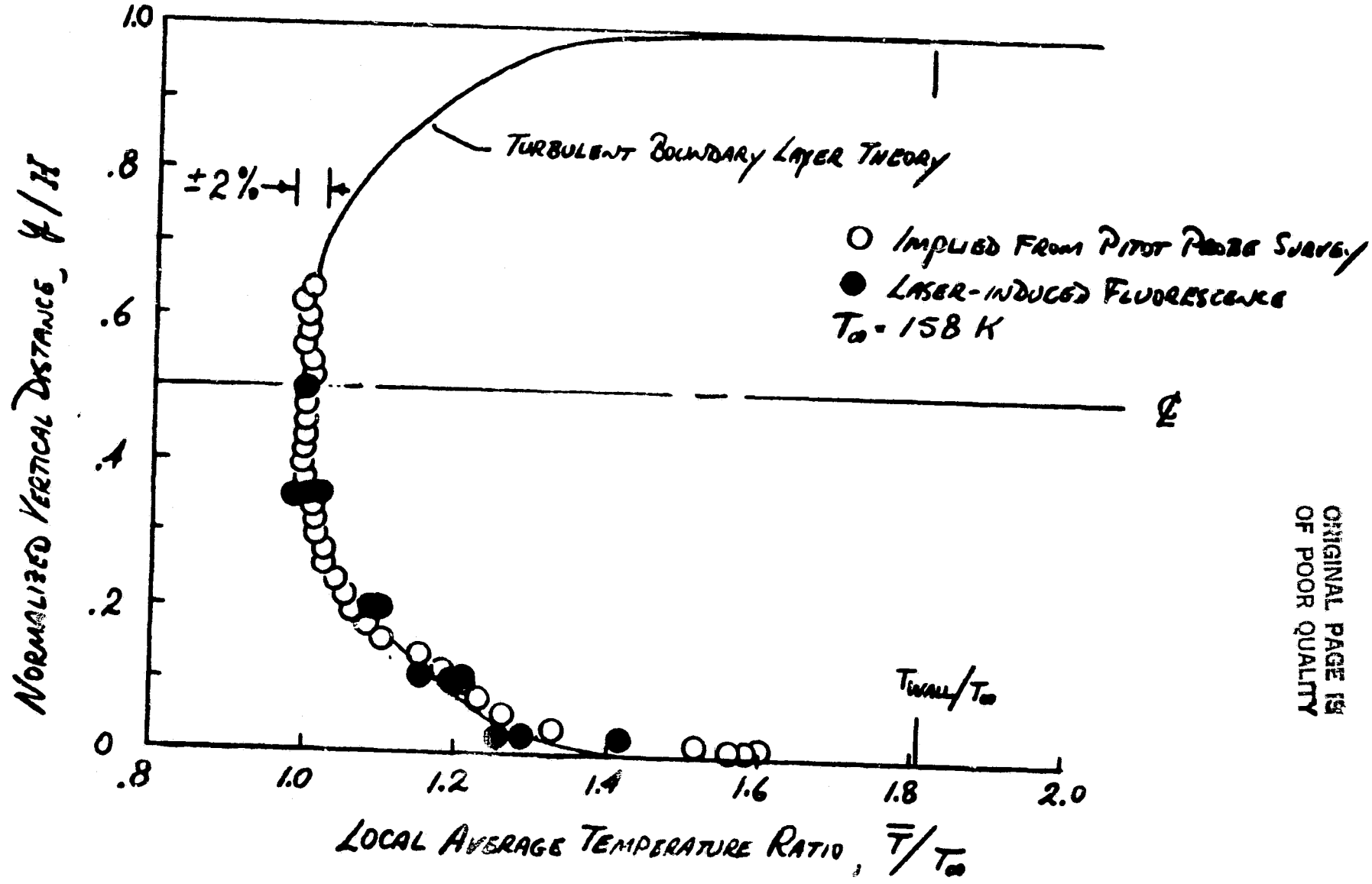

FIGURE 4. AVERAGE TEMPERATURE DISTRIBUTION IN A MACH 2.0 CHANNEL

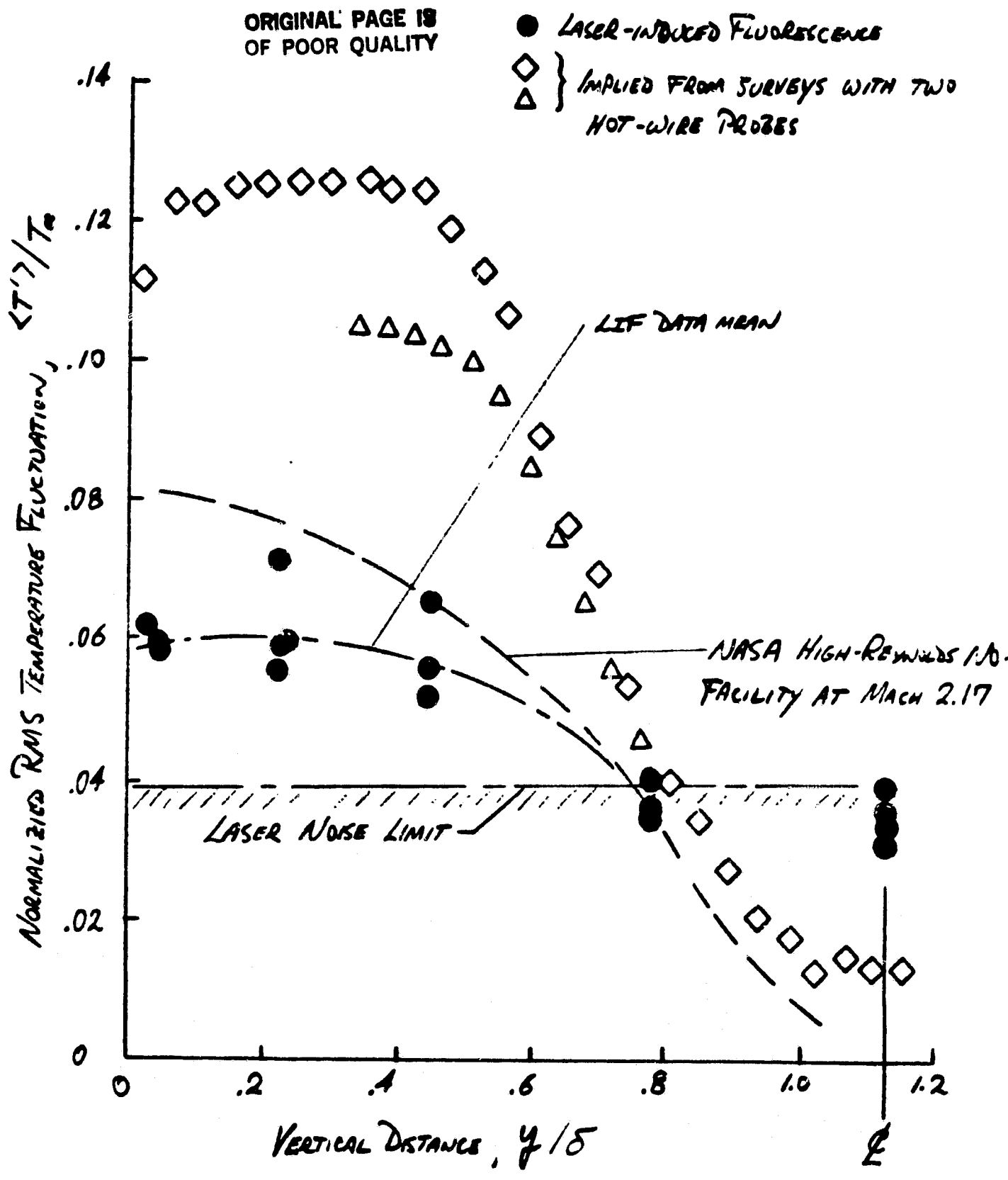

FIGURE 5. TEMPERATURE FLUCTUATIONS IN A MACH 2.0 CHANNEL

REFERENCE 3

Optical Stark Effect in the Two-Photon Spectrum of NO

Winifred M. Huo[a*], Kenneth P. Gross[b*#], and Robert L. McKenzie[c]

[a]Radiation Laboratory, University of Notre Dame, Notre Dame, IN 46556

[b]Stanford University, Stanford, CA 94305

[c]NASA Ames Research Center, Moffett Field, CA 94035

Abstract

A large optical Stark effect has been observed in the two-photon spectrum $X^2\Pi \rightarrow A^2\Sigma^+$ in NO. This is explained as a near resonant Stark effect where the upper state of the two-photon transition is perturbed by higher-lying electronic states through the laser field. A theoretical analysis is presented along with coupling parameters determined from ab initio wavefunctions. The agreement between the experimental and synthetic spectra is good.

In this letter we report the first quantitative determination of the optical Stark effect in a molecular two-photon electronic transition. Optical Stark effects have previously been observed in resonant two-photon atomic transitions[1] and in resonant multiphoton ionization of atoms.[2—5] However, the electronic spectra of molecules are more complex due to the increased density of states. Molecular Stark effects are expected to be more easily observed, especially in multiphoton transitions where high laser intensities are used. To date, few such studies have been reported. To our knowledge, they have been observed by Otis and Johnson[6] in the multiphoton ionization of NO, and by Srinivisan et al[7] in two- and three-photon resonant sum frequency mixing in H_2.

Two of us[8,9] have developed a laser induced fluorescence technique for temperature diagnostics in low temperature gas flows seeded with small concentrations of NO. The method relies on the two-photon excitation of two selected ro-vibronic transitions in the NO $\gamma(X^2\Pi, v''=0 \rightarrow A^2\Sigma^+, v'=0)$ band. Due to the inherently weak two-photon interaction, high laser power densities are required to provide adequate signal levels. However, an anomalously large Stark broadening was observed in the two-photon spectrum, even at moderate power levels. The broadening, which introduces additional uncertainties in the diagnostic method, is avoided by using reduced laser power levels. We have, however, studied the Stark effect in some detail in order to understand the source of the large broadening.

The experimental arrangement used is similar to that described in Ref. 9. Selected regions of the $\gamma(0,0)$ two-photon fluorescence excitation spectrum were scanned with a dye laser pumped by a Nd:YAG laser operated at 10Hz. A linearly polarized beam was

generated with 5 nsec pulse duration, average linewidth of $\approx 0.2 - 0.3\ cm^{-1}$, and energies of a few mJ. The beam intensity distribution was spatially and temporally nonuniform and varied from pulse to pulse. A large fraction of the beam was focussed into a sample cell for the Stark measurements while $\approx$ 10% of the beam was split off and loosely focussed into a reference cell to provide a simultaneous spectrum with negligible Stark broadening. The broadband fluorescence from each cell was collected at 90° and imaged onto a photomultiplier through an aperture that limited observation to a 1-mm path length at the focal point. Signals were integrated and averaged with a boxcar integrator.

An example of the broadening observed is shown in Fig. 1a in a spectral region of well separated transitions. The upper trace was taken using an average laser intensity of $\approx 3\ GW/cm^2$. The lower trace, recorded simultaneously with a reduced laser power level, shows a spectrum where the Stark effect is negligible. The upper spectrum displays an asymmetric shift to the blue for both the $S_{11} + R_{21}(20\frac{1}{2})$ and $S_{21}(16\frac{1}{2})$ transitions. The M levels which are split by the laser field are not resolved and the splitting appears in the spectrum as a broadening 3 — 4 cm^{-1} wide. Additionally the peak height ratio of the two peaks is reversed at high laser power. Fig. 2 shows a plot of the full width at half height (FWHM) of the $S_{11} + R_{21}(20\frac{1}{2})$ and $S_{11} + R_{21}(7\frac{1}{2})$ lines as a function of the average laser energy. The width is linearly proportional to the pulse energy, indicating that a quadratic Stark effect is observed. The intercept at zero energy corresponds to the two-photon convoluted laser width and Doppler width.

To account for the observed Stark effect quantitatively, both level shifts and widths induced by the optical field need to be considered. The likely cause of the large splitting

is a near resonant Stark effect. A survey of the one-photon and multiphoton spectroscopic data of NO[10—16] shows that, at the laser frequencies used for the two-photon X → A transition, each rotational level of the A state is near one-photon resonant with a J level of some high lying discrete electronic state. The observed splitting can be attributed to a near resonant one-photon coupling via the Stark field, i.e., a quadratic Stark effect. In addition to the splitting, a width is also introduced by the Stark field. While near-resonant one-photon coupling with discrete states does not introduce any significant width, the A state can be two-photon coupled with the continuum, which is enhanced by the near resonant one-photon step. This additional width, due to a quartic Stark effect, can also be termed the two-photon ionization width. Since this width is strongly M dependent, the term Stark width appears more appropriate in the present case.

An important factor in determining the magnitude of the observed Stark effect is the resonance energy gap, G, which is the difference between the energies of the perturbing state and the A state + photon energy. The A state, being the first excited doublet state, has all perturbing levels lying above it. From the experimental data in the region near one photon resonance (≈ 450 nm) with the A state,[10,17] we have identified the strongest perturbing level of the $S_{11}+R_{21}(20\frac{1}{2})$ branch to be $B^2\Pi$, v=25, and for the $S_{21}(16\frac{1}{2})$ branch, $K^2\Pi$, v=1. The resonant energy gaps were calculated with expressions appropriate for intermediate coupling between Hund's case (a) and (b),[18] using spectroscopic parameters derived from experiment.[17,19] The frequencies of the Stark field used in the calculation are the laser frequencies for the two-photon transitions at low field. The resonance energy gaps are given in Table I. For all three A state rotational levels considered, the smallest G is $< 11\ cm^{-1}$. It is not surprising that large Stark shifts are observed.

We have calculated the Stark shifts in NO by solving the time-dependent Schrödinger equation with the A state coupled to six rotational levels of the $B^2\Pi$ or $K^2\Pi$ state via dipole interactions; i.e., $J=J_A+1$, J_A, J_A-1 for each of the two spin components F_1 and F_2 of the perturbing state. Since near resonant Stark effects apply only to the $A^2\Sigma^+$ state, we have neglected contributions from the $X^2\Pi$ state. In general, the time-dependent Schrödinger equation [20]

$$i\frac{\delta\Psi}{\delta t} = [H_o + V(\vec{r},t)]\Psi, \tag{1}$$

with H_o the molecular Hamiltonian and $V = -\vec{\mu}\cdot\vec{\mathcal{E}}\cos\omega t$, cannot be solved using stationary state methods. However, in the restricted part of the Hilbert space with only bound eigenstates of H_o resonantly or near resonantly coupled, and with their natural lifetimes neglected, we can recast Eq. (1) into the form of a secular equation.[21] Thus for a state A coupled to a set of bound states I,J through the potential V, we have

$$\mathcal{G} + \mathcal{V} - \alpha = 0 \tag{2}$$

where $G_{AA} = 0$, $G_{IJ} = (E_I - E_A - \hbar\omega)\delta_{IJ}$, $V_{AA} = 0$, and

$$V_{AI} = -\tfrac{1}{2}\mathcal{E}\,\mu_{AI}\,\mathcal{R}(J_A, J_I, S_A, S_I, M) \tag{3}$$

Also, we set $V_{IJ} = 0$ when I and J belong to the same vibronic state because their interaction is nonresonant. μ_{AI} is the dipole transition moment between A and I and $\mathcal{R}$ is a rotational line shift factor. Associated with each eigenvalue α_N there is a stationary wavefunction $\Psi_N(\vec{r},t)$ which is a solution of Eq. (1)

$$\Psi_N(\vec{r},t) = [B_{NA}\Phi_A(\vec{r}) + \sum_I B_{NI}\Phi_I(\vec{r})]e^{-(E_A-\alpha_N)t} \tag{4}$$

where Φ_A and Φ_I are eigenfunctions of H_o. The wavefunction $\Psi(\vec{r},t)$, satisfying the boundary condition that $\Psi(\vec{r},0) = \Phi_A(\vec{r})$, is a linear combination of the Ψ_N's.

$$\Psi(\vec{r},t) = \sum_N C_N \Psi_N(\vec{r},t) \tag{5}$$

The correct wavefunction for our problem is nonstationary and oscillates among the Ψ_N's depending on time. For the case of two-state coupling (Autler-Townes effect[22]), our result agrees with that obtained previously in closed form.[23]

While $\Psi(\vec{r},t)$ is oscillatory, the laser probes only one of its components. In this experiment, the probe field and the Stark field are identical and are always tuned to the component of $\Psi(\vec{r},t)$ with α closest to zero, which we designate Ψ_o. The eigenvalue α_o then corresponds to the Stark shift observed. Other components of Ψ_N, with larger α_N's, are not observed because α_N is simultaneously shifted as the frequency of the probe laser (Stark field) is tuned.

Eq. (2) is solved separately for each M level. The parameters used in the calculation are the resonance energy gap G and the coupling potential V. Since the experiment requires the Stark and probe frequencies to be equal, Eq. (2) was solved iteratively until the two frequencies agreed. The determination of the rotational line shift factor, R, depends on the Hund's coupling case for which the pair of molecular eigenstates A and I belong. The electronic states of NO belong to Hund's case (a), (b), or intermediate between the two cases. Assuming a single frequency linearly polarized light source, we find for the general case of intermediate coupling,

$$R(J_A, J_I, S_A, S_I, M) = \left(\frac{2J_A+1}{2J_I+1}\right)^{\frac{1}{2}} C(J_A\,1\,J_I, M\,0\,M)$$

$$\times\left[\sum_{\Omega_A=-\frac{1}{2}}^{\frac{1}{2}}\sum_{\Omega_I=-\frac{1}{2}}^{\frac{1}{2}} < A^2\Sigma^+, J_A \pm \tfrac{1}{2} \mid A^2\Sigma^+, \Omega_A > C(J_A 1 J_I, \Omega_A 1 \Omega_I) <^2 \Pi, J_I \pm \tfrac{1}{2} \mid^2 \Pi, \Omega_I >\right] \tag{6}$$

Here Rose's definition of Clebsch-Gordan coefficients are used.[24] For $^2\Sigma^+$ and $^2\Pi$ states, $J - \frac{1}{2}$ applies to the F_1 spin component and $J + \frac{1}{2}$ to the F_2 component. The expression of $< \beta, J \pm \frac{1}{2} \mid \beta, \Omega >$ in terms of the spectroscopic parameters of the state β can be found in Bennett.[12]

The two-photon rotational line strength $S(J_X, J_A, S_X, S_A, M)$ between individual M levels of the $X^2\Pi$ and $A^2\Sigma^+$ states determines the shape of the Stark spectrum. The M-dependent line strength can be deduced from the unresolved two-photon rotational line strength of Halpern et al,[25] $S(J_X, J_A, S_X, S_A)$, valid for intermediate coupling

$$S(J_X, J_A, S_X, S_A, M) = \frac{5 \mid C(J_A 2 J_X, M 0 M) \mid^2}{2J_X + 1} S(J_X, J_A, S_X, S_A). \tag{7}$$

The Stark width is introduced by the interaction of the wavefunction Ψ_o with the ionization continuum via the radiation field and is expressed by

$$\Delta\Gamma = \frac{\pi}{2}\sum_{\lambda} |< \Phi_{c,\lambda} \mid \vec{\mu} \cdot \vec{\mathcal{E}} \mid \Psi_o >|^2 \tag{8}$$

The continuum states are evaluated at energy $E_C = E_A + 2\hbar\omega$, and the subscript λ sums over all degenerate quantum numbers. The Stark width $\Delta\Gamma$ is also M dependent through rotational factors similar to R. The energy shift associated with the coupling to the continuum is found to be numerically small for NO and will not be discussed further here.

The vibronic transition moments μ_{AI} necessary to evaluate the Stark effects have been calculated using ab initio wavefunctions. The electronic wavefunctions were calculated using a large Slater-type basis set containing Rydberg functions. Complete-active-space SCF calculations[26] (CASSCF) were carried out for the $A^2\Sigma^+$ state, followed by multi-reference first order configuration-interaction (CI) calculations[27] for both $^2\Sigma$ and $^2\Pi$ symmetries. The vibrational wavefunctions are numerical solutions of the Schrödinger equation of vibration. Transition moments between the B, $K^2\Pi$ states and the ionization continuum were calculated using the Stieltjes imaging method[28] from discretized CI wavefunctions.

The Stark shifts and widths of the three rotational levels of the $A^2\Sigma^+$ state have been calculated for the experimental field intensity I_{AV} of 3 GW/cm^2 using a chaotic field model for the photon statistical behavior.[29] Their values are shown in Table II for representative M levels. Both the shifts and widths are strongly M dependent due to a dominant M^2-dependent term in V_{AI}. Uncertainties in both the energy gaps and transition moments contribute to the error in the theoretical Stark parameters. The J dependence of the rotational constants used in the calculation of G are not well known experimentally and constitute the largest source of uncertainty in its determination. While it is difficult to determine the error associated with ab initio transition moments, calculations of X to A one-photon and two-photon transition probabilities[30] indicate that the bound-bound transition moments should be reliable. The bound-free transition moments are subjected to much larger errors, resulting in calculated widths that are less reliable than the shifts.

A synthetic Stark broadened two-photon spectrum of NO has been generated using

the calculated parameters and is presented in Fig. 1b. At a given probe frequency in the synthetic spectrum, all transitions which contributed to the intensity were convoluted with the laser and Doppler widths using a Voigt function. The laser width was assumed to be composed of both probe and Stark fields, and an effective single Gaussian width of 0.5 cm^{-1} was used. Additionally, the spatial non-uniformity in the beam intensity was modelled by using a distribution of intensities instead of a single average value. The synthetic spectrum was not sensitive to the particular intensity distribution used, but had a smoother line-shape profile than the spectrum generated with a single value of I'_{AV}. The vertical lines in Fig. 1b represent the calculated positions of the Stark-shifted M level transitions at I_{AV}.

Comparing the synthetic and experimental spectra, we find overall agreement. Both spectra show asymmetric shifts to the blue and a peak height reversal from the low field case. The asymmetry is the result of M-dependent blue shifts and their intensity distributions. The individual Stark widths smooth the line shape for high M transitions. There are, however, some discrepancies between the two spectra. On the high frequency side of the $S_{11} + R_{21}(20\frac{1}{2})$ transition, the synthetic spectrum shows more curvature. Also, the $S_{12}(16\frac{1}{2})$ transition is narrower than the $S_{11} + R_{21}(20\frac{1}{2})$ transition in the synthetic spectrum while their widths (FWHM) appear to be approximately the same experimentally. These differences probably are due to uncertainties in the theoretical Stark parameters discussed earlier. However, the general agreement between the experimental and synthetic spectra indicates that our account of the Stark effect in NO is correct.

References

* Mailing address; NASA Ames Research Center, Moffett Field, Ca. 94035.

Current affiliation: Polyatomics Research Institute, Mountain View, CA 94043.

[1] P. F. Liao and J. E. Bjorkholm, Phys. Rev. Lett. 34, 1 (1975); J. E. Bjorkholm and P. F. Liao , Opt. Commun. 21, 132 (1977).

[2] B. Held, G. Mainfray, C. Manus, J. Morellec, and F. Sanchez, Phys. Rev. Lett. 30, 423 (1973).

[3] J. Morellec, D. Normand, and G. Petite, Phys. Rev. A14, 300(1976).

[4] P. Agostini, A. T. Georges, S. E. Wheatley, P. Lambropoulos, and M. D. Levensen, J. Phys. B11, 1733 (1978).

[5] P. H. Tjossum and T. A. Cool, Chem. Phys. Lett 100, 479 (1983).

[6] C. E. Otis and P. M. Johnson, Chem. Phys. Lett 83, 7? (1981).

[7] T. Srinivasan, H. Egger, H. Pummer, and C. K. Rhodes, IEEE Quantum Electronics , (1983).

[8] R. L. McKenzie and K. P. Gross, Applied Optics, 20, 2153 (1981).

[9] K. P. Gross and R. L. McKenzie, Optics Letters 8, 368 (1983).

[10] E. Miescher and K. P. Huber, *Spectroscopy*, M. T. P. International Review of Science Physical Chem. Ser. Two, 3, D. A. Ramsay, Ed. (1976).

[11] K. P. Gross and R. L. McKenzie, J. Chem. Phys. 76, 5260 (1982) and unpublished work.

[12] T. Ebata, H. Abe, M. Mikami, and M. Ito, Chem. Phys. Lett 86, 445 (1982).

[13] T. Ebata, T. Imajo, N. Mikami, and M. Ito, Chem. Phys. Lett. 89, 45 (1982).

[14] T. Ebata, N. Mikami, and M. Ito, J. Chem. Phys. 78, 1132 (1983).

[15] E. R. Sirkin, M. Asscher, and Y. Haas, Chem. Phys. Lett. 86, 265 (1982).

[16] T. C. Steimle and H.-T. Liou, Chem. Phys. Lett. 100, 300 (1983).

[17] A. Lagerqvist and E. Miescher, Can. J. Phys. 44, 1525 (1966).

[18] R. J. M. Bennett, Mon. Not. R. Astr. Soc. 147, 35 (1970).

[19] R. Gallusser and K. Dressler, J. Chem. Phys. 76, 4311 (1982).

[20] Unless explicitly stated otherwise, atomic units with $e = m_e = \hbar = 1$ are used.

[21] W. M. Huo, K. P. Gross, and R. L. McKenzie, unpublished work.

[22] S. H. Autler and C. H. Townes, Phys. Rev. 100, 703 (1955).

[23] L. D. Landau and E. M. Lifshitz, *Quantum Mechanics*, Pergamon Press (London, 1958), p. 143.

[24] M. E. Rose, *Elementary Theory of Angular Momentum*, John Wiley and Sons, New York, (1957).

[25] J. B. Halpern, H. Zacharias and R. Wallenstein, J. Mol. Spectrosc. 79, 1 (1980).

[26] P. E. M. Siegbahn, A. Heiberg, B. O. Roos, and B. Levy, Physica Scripta 21, 1 (1980).

[27] H. F. Schaefer III, R. A. Klemm, and F. E. Harris, Phys. Rev. 187, 137 (1969).

[28] M. R. Hermann and P. W. Langhoff, J. Math. Phys. 24, 541 (1983).

[29] P. Zoller and P. Lambropoulos, J. Phys. B13, 69 (1980); P. Lambropoulos, (private communication).

[30] W. M. Huo, unpublished work.

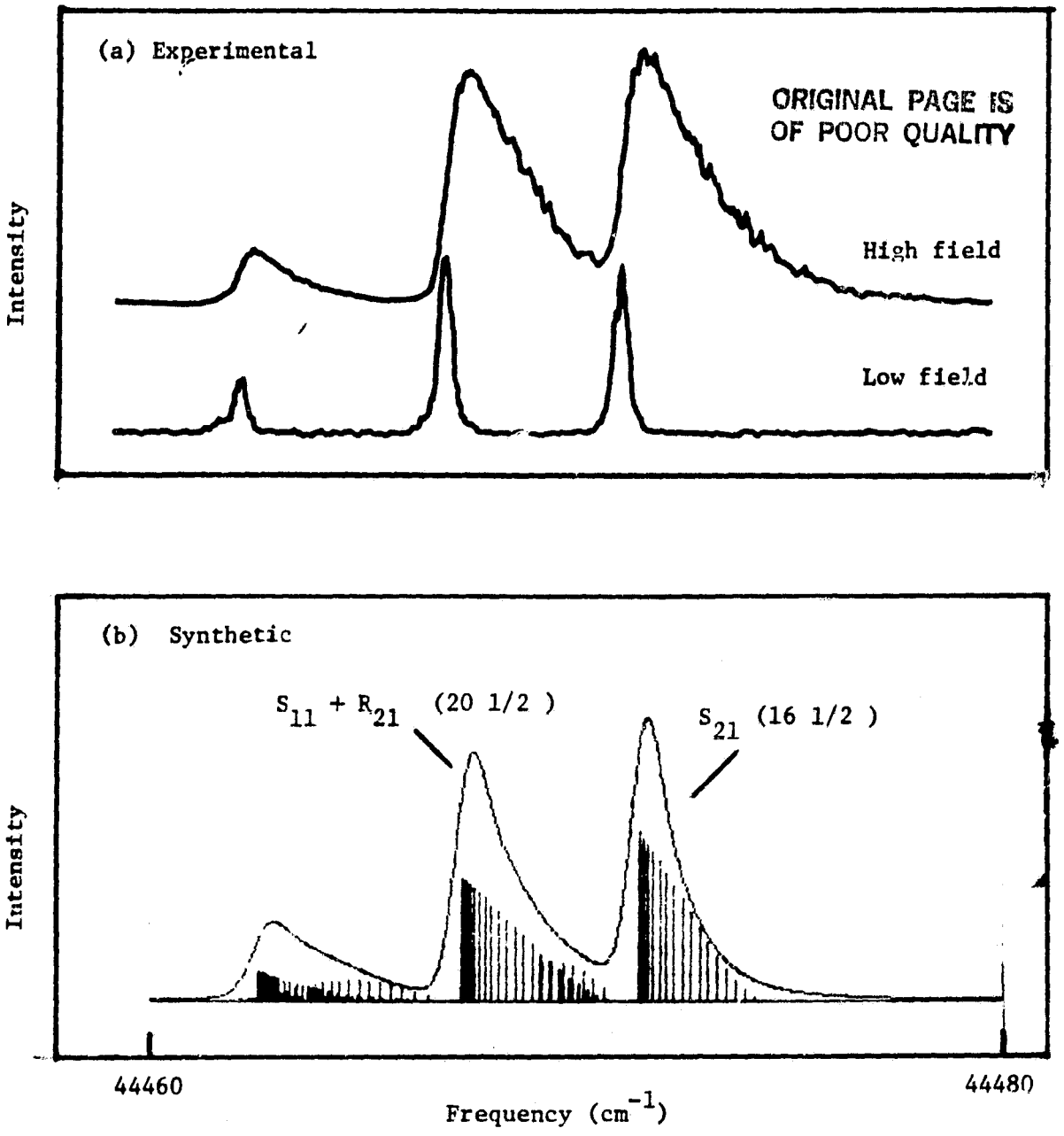

Figure 1 (a). Experimental two-photon spectrum of NO, $X^2\Pi$, $v''=0 \rightarrow A^2\Sigma^+$, $v'=0$, $S_{11}+R_{21}(20\frac{1}{2})$ and $S_{21}(16\frac{1}{2})$ transitions. The upper trace (high field) was taken using 2 mJ pulse energy and a focused beam diameter $\approx$ 100 - 150 μ. The corresponding parameters for the lower trace are: 0.2 mJ energy and $\approx$ 300 μdiameter. (b). Synthetic spectrum of the same transitions generated using the experimental high field parameters.

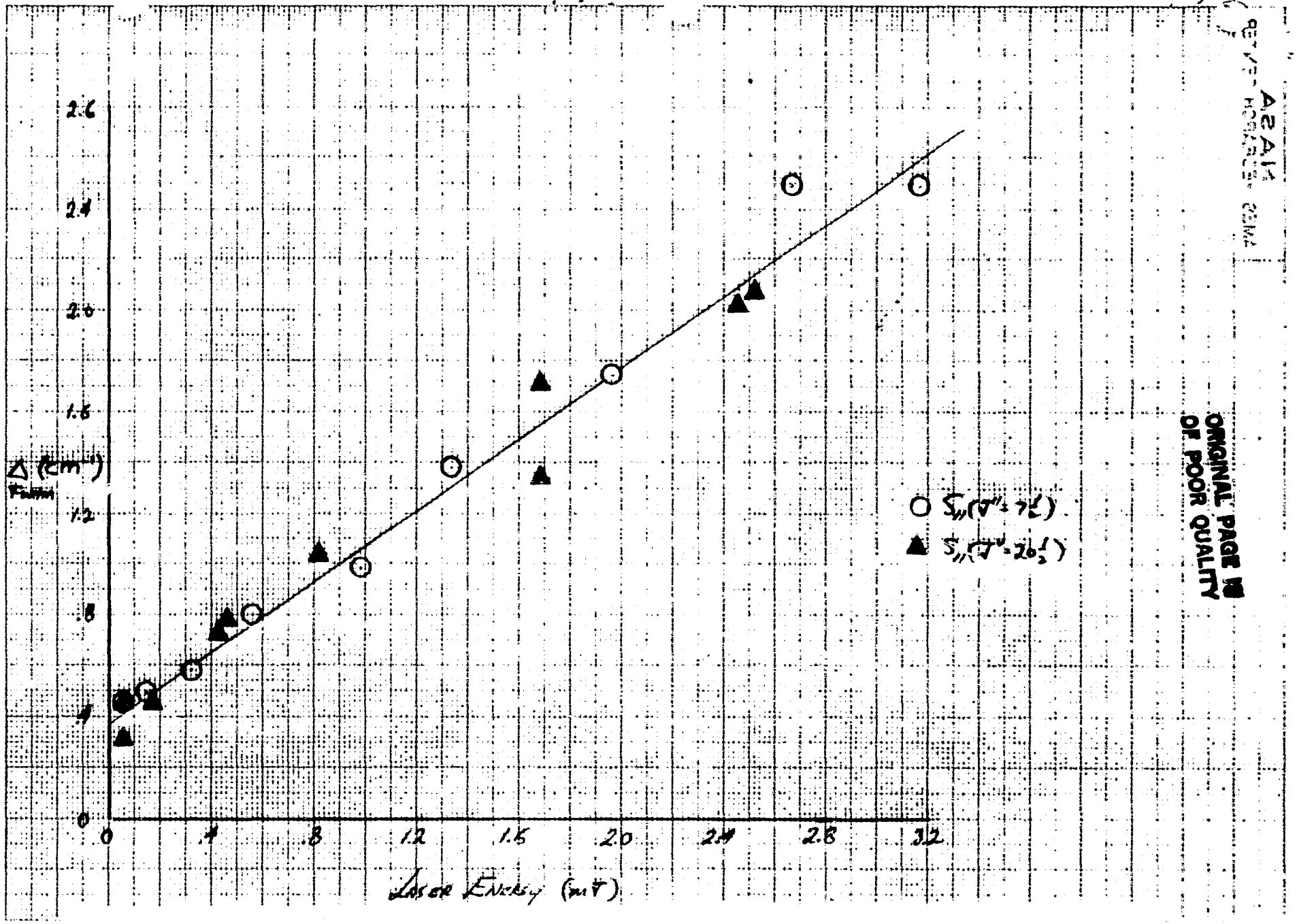

Figure 2. Linewidth (FWHM) of the $S_{11} + R_{21}(20\frac{1}{2})$ and $S_{11} + R_{21}(7\frac{1}{2})$ lines as a function of laser energy. Focussed beam diameter was $\approx 300\ \mu$.

Table I. Energy gap G_{AI} in cm^{-1} used in the calculation of Stark parameters[a]

Perturbing $^2\Pi$ state	$A^2\Sigma^+$, v =0 (a) F_1, $J_A=22\frac{1}{2}$	(b) F_2, $J_A=21\frac{1}{2}$	(c) F_2, $J_A=18\frac{1}{2}$
F_1, $J=J_A+1$	47.7	-10.8	-66.8
F_1, $J=J_A$	-10.8	-65.7	-119.5
F_1, $J=J_A-1$	-65.7	-118.6	-169.9
F_2, $J=J_A+1$	95.8	39.6	53.1
F_2, $J=J_A$	39.6	-13.8	-7.0
F_2, $J=J_A-1$	-13.8	-64.8	-64.2

[a] For columns a and b, the perturbing $^2\Pi$ state is $B^2\Pi$, v=25. For column c it is $K^2\Pi$, V=1.

Table II. Stark shifts(cm^{-1}) and widths(cm^{-1}) calculated for three rotational levels of the $A^2\Sigma^+$, v=0 state at I_{AV} = 8 GW/cm^2

	F_1, J=22½		F_2, J=21½		F_2, J=18½	
M	Shift	Width	Shift	Width	Shift	Width
½	0.00	0.05	-0.01	0.04	-0.06	0.02
5½	0.46	0.12	0.38	0.10	0.50	0.27
10½	1.42	0.22	1.28	0.21	1.58	0.57
15½	2.62	0.29	2.51	0.31	2.84	0.81
20½	3.93	0.35	3.94	0.40		